17th World Conference on Earthquake Engineering, 17WCEE
Sendai, Japan - September 13th to 18th 2020

A NOVEL PROCEDURE OF PROBABILISTIC SEISMIC PERFORMANCE EVALUATION FOR A LIGHT-FRAME WOOD BUILDING

Jixing Cao[(1)], Haibei Xiong[(2)], Lin Chen[(3)]

[(1)] *Ph. D candidate, Department of Disaster Mitigation for Structures, Tongji University, Shanghai, 200092, China, caojixing1991@163.com*
[(2)] *Professor, Department of Disaster Mitigation for Structures, Tongji University, Shanghai, 200092, China, xionghaibei@tongji.edu.cn,*
[(3)] *Ph. D candidate, Department of Disaster Mitigation for Structures, Tongji University, Shanghai, 200092, China, 1710742@tongji.edu.cn*

Abstract

The probabilistic seismic performance evaluation for light-frame wood buildings (LFWBs) is vital for the design guidance and rehabilitation of the existing buildings. This paper develops a framework of probability seismic assessment conjoined with model updating technique. It involves the model updating and seismic performance assessment, where the cubature Kalman filter (CKF) is adopted to update the finite element (FE) model using available experimental data, and the fragility analysis and limits state analysis are then implemented based on the updated FE model. The CKF assumes that the prior probability density function of the state vector is Gaussian distribution and the cubature rule is utilized to obtain the estimates of mean and covariance given the known input and output. The proposed framework is applied to the LFWB case. According to the experiment of a one-story full-scale LFWB under the cyclic test, an FE model whose nonlinearity is governed by the spring elements is created. Due to the inaccurate model assumption and parameter uncertainty, the CKF that characterizes modeling uncertainties associated with the underlying structural system is utilized to update the FE model. The updated FE model is taken as an element to assemble different configurations ranging from one story to six-story. The fragility analysis and limited state analysis is fulfilled to assess the seismic performance. The obtained information can be further used to loss estimation and expand the knowledge of engineering decision-making for seismic risk evaluation of LFWB.

Keywords: light-frame wood building; cubature Kalman filter; model updating; probabilistic seismic performance evaluation;

1. Introduction

The light-frame wood buildings (LFWBs) are an accessible residential construction in North America because of its aesthetics and constructability. In recent earthquakes, this type of structures suffered from severe damage and quantifies of property loss [1][2]. These unexpected destructions drive some researchers to study the seismic performance of structures. For assessing the structural response at different seismic intensity levels, a robust and computationally efficient model is necessary [3][4]. The model updating technique provides a useful tool to obtain a reliable model. It is essentially a process of adjusting model parameters to narrow the gap between model estimation and experimental result by some optimization algorithms. Recently, the Bayesian method gains popularity for the reason that it not only treats the parameter identification as a probabilistic framework [5], but also characterize modeling uncertainties following the underlying structural system [6]. For the nonlinear filtering problems based on the Bayesian framework, several Gaussian approximation filters that estimates the mean vector and covariance matrix of the random vector by defining a set of deterministically chosen sample points, have been developed, such as the unscented Kalman filter, the CKF, and the Gauss–Hermite quadrature filter. Among these methods, the CKF has better numerical stability than the unscented Kalman filter and has less computational complexity compared with the Gauss-Hermite filter [7]. Therefore, the CKF is employed as a model updating technique in this study to update the FE model with experimental data. The main contribution of this paper is to develop a framework that combines the model updating technique with seismic probability assessment. The

model updating technique aims to obtain a reliable FE model, and the seismic performance is evaluated based on the calibrated FE model, providing insight into the seismic risk assessment.

2. The framework of probabilistic seismic performance evaluation incorporated with model updating technique

2.1 Model updating for the FE model using Cubature Kalman filter

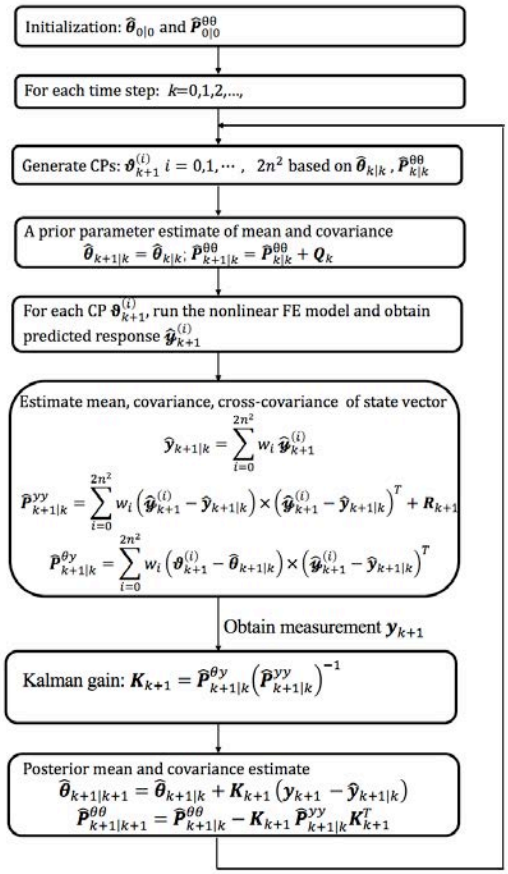

Fig. 1 Procedure of model updating for the nonlinear FE model using CKF

The Cubature Kalman filter (CKF) is used to solve the estimation problem in this paper. It assumes that the posterior probability density function of state vector is Gaussian distribution and the cubature rule is employed to estimate its mean and covariance matrix by defining a set of deterministically chosen sample points. For the case of joint parameter-state estimation, the state vector is usually augmented to the unknown parameters. However, an extensive literature has demonstrated that the FE model can capture the structural response with reasonable accuracy if the model parameters are well-calibrated [8]. Then the predicted response can be obtained from the FE model, making them discard in the state vector. The joint state-parameter estimation problem can be changed to the parameter estimation issue, which means only the unknown parameters are considered in the state equation, i.e.,

$$\boldsymbol{\theta}_{k+1} = \boldsymbol{\theta}_k + \boldsymbol{\gamma}_k \tag{1}$$

in which the subscript k denotes the time step, $\boldsymbol{\theta}_{k+1}$ is model parameter vector to be identified and $\boldsymbol{\gamma}_k$ is Gaussian white noise process.

The measurement equation is then constructed by the FE model yielding any desired structural response, which can be mathematically formulated as

$$\boldsymbol{y}_{k+1} = \boldsymbol{h}_{k+1}(\boldsymbol{\theta}_{k+1}, \boldsymbol{u}_{1:k+1}) + \boldsymbol{v}_{k+1} \tag{2}$$

where $\boldsymbol{h}(\cdot)$ is the nonlinear FE model, $\boldsymbol{v}_{k+1}$ is Gaussian white noise and $\boldsymbol{y}_{k+1}$ is the response.

The Equation (1) and (2) involves a state-space model, in which the Equation (1) is corresponding to the evolution of parameter vector and the Equation (2) gives a correction for the FE prediction. The objective of parameter estimation in the nonlinear state space dynamic system is to estimate the mean and covariance of the parameters using the available experimental data that can be solved by the CKF. Fig. 1 summarizes the procedure of nonlinear FE model updating using the CKF.

2.2 Procedure of probabilistic seismic performance evaluation for light-frame wood buildings

An accurate and reliable FE model is a precondition for analyzing the structure behavior, such as the internal force and displacements of structures in several limit states, or predicting vibration responses due to the dynamic load of earthquakes. When the FE model is calibrated with the real data, it can be utilized to assess the structural seismic performance. The probabilistic seismic assessment consists of three main components [9]: fragility analysis, seismic hazard analysis and limit state analysis. A detailed procedure for the probabilistic seismic assessment is explained as follows.

The fragility analysis is to estimate the failure probabilities (e.g., probability of exceeding a specific drift, damage, or collapse threshold) as a function of intensity measures (IM). It is usually assumed that the fragility curve is described by a lognormal distribution function, i.e.,

$$P(LS|IM = x) = \Phi\left(\frac{ln(x/\theta)}{\beta_c}\right) \tag{3}$$

where $P(LS|IM = x)$ is probability of the limit state (LS) given a ground motion with $IM = x$; $\Phi(\cdot)$ is the standard normal cumulative distribution function; θ is the median of fragility function; β_c is the uncertainty related to seismic demand and structural capacity,

$$\beta_c = \sqrt{\sigma_\theta^2 + \beta_{SC}^2} \tag{4}$$

in which σ_θ and β_{SC} are the uncertainties in seismic demand and structural capacity, respectively.

The limit state analysis is the estimate of probabilities of different levels of damage state risks, serving as a risk metric during the estimation of expected losses. It is usually assumed that both seismic intensity demand (Q) and structural capacity (R) are random variables, the LS occurs if R is less than Q, which can be expressed in the probability logic,

$$P_{LS} = P[R < Q] = \sum_x P[LS|\mathrm{Q} = x]P[Q = x] \tag{5}$$

in which $P[LS|Q = x]$ denotes the fragility probability and $P[IM = x]$ represents the seismic hazard. They are two essential ingredients of seismic risk assessment.

Seismic hazard analysis investigates the site seismic properties and gives the annual exceedance probability of a specific level of earthquake intensity, which can be calculated by

$$H[x] = k_0 x^{-k} \tag{6}$$

where k_0 and k are scale and shape parameters depending on the site of buildings.

When submitting Eqs. (3), (4), (6) into (5), the limit state annual exceedance probability can be approximately calculated as [10],

$$P_{LS} \approx \left(k_0 m_R^{-k}\right)\exp[(k\beta_c)^2/2] \tag{7}$$

The probabilistic seismic performance assessment involves the fragility analysis and limit state analysis, providing information in loss analysis and public decision-making. The framework of model updating techniques embedded in the seismic performance assessment is presented in Fig. 2. In the first stage, the model updating technique aims to obtain a reliable and accurate FE model, which is then used for the next stage analysis. In the second stage, the calibrated FE model is utilized to implement the probabilistic seismic performance assessment, expanding the knowledge of engineering decision-making for seismic risk evaluation.

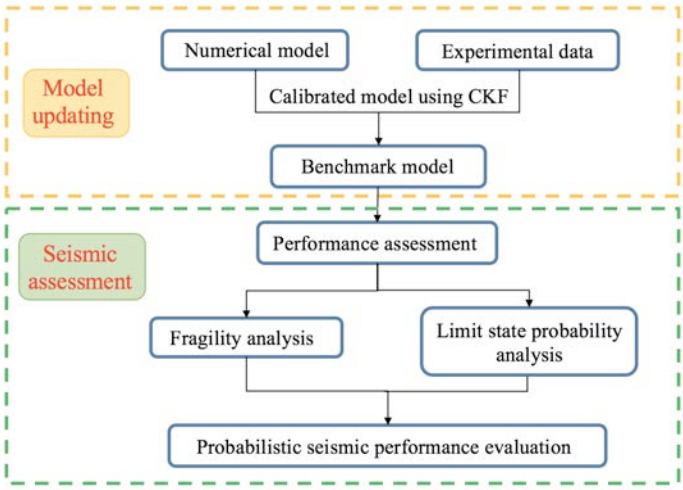

Fig. 2 Framework of the probabilistic seismic performance evaluation incorporated with model updating technique

3. Numerical model for light-frame wood buildings

To investigate the mechanical performance of WFC, a series of three-dimensional (3D) full-scale structures subjected to cyclic loading were carried out at the State Key Laboratory of Disaster Reduction in Civil Engineering, Tongji University, China [11]. The full-scale test model (Fig. 3(a)) was 2440 mm height, consisting of four shear walls with 6100 mm×6100 mm. The schematic of setup was presented in Fig. 3(b), where the lateral cyclic loading was applied to the structure through the hydraulic actuator. The cyclic loading protocol was displacement control followed by the American Society for testing and materials E2126 [12].

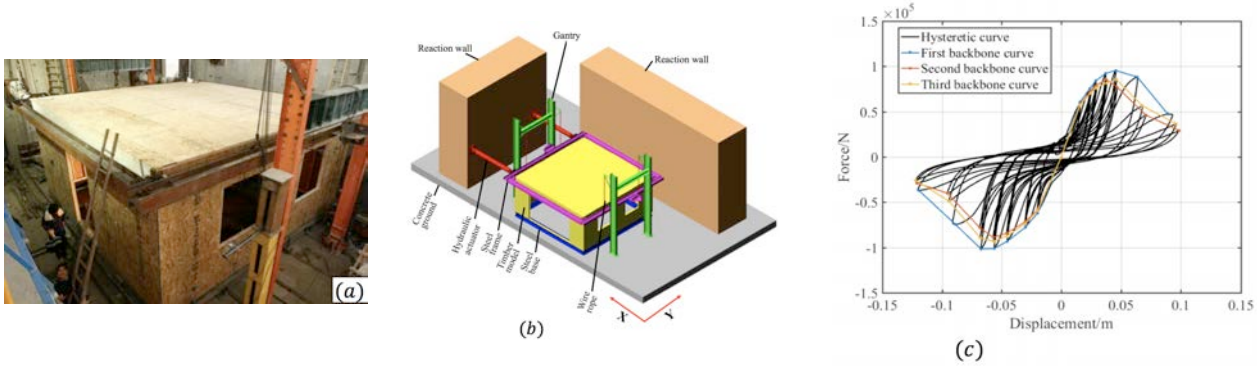

Fig. 3(a) Overview of the test model, (b) sketch of the whole setup, (c) test hysteretic curve.

The hysteretic response obtained from test exhibiting highly nonlinear fashion, such as stiffness and strength degradation, as shown in Fig. 3(c). The hysteresis loops manifested symmetric, and thinner near the center than at the end of the loops attributing to the loss of stiffness. This pinching phenomenon was owing to the nails surrounded by a cavity caused by crushing of the surrounding medium during the previous loading cycle.

To simulate the hysteretic behavior of LFWB, a simplified model of LFWB is developed in the OpenSees platform [13]. It is assumed that a single shear wall is built with a concept of the concentrated plasticity, where the nonlinearity is controlled by the spring elements, as shown in Fig. 4. The backbone of a shear wall is modeled with the "ElasticBeamColumn" element that only transfers compression and tension force. The joint is connected by "zeroLength" elements assigned with very small stiffness values so that the columns and beams do not attract significant moments. The truss elements are utilized to link spring elements to the diagonals for simulating the whole area of a shear wall. The spring element is assigned to the

uniaxial material Pinching4 that is widely used in a timber structure. Fig. 4(c) depicts the cyclic rule of Pinching4, where the pinching, cyclic stiffness, and strength degradation are taken into account. An elaborate description of the Pinching4 can be referred to [14].

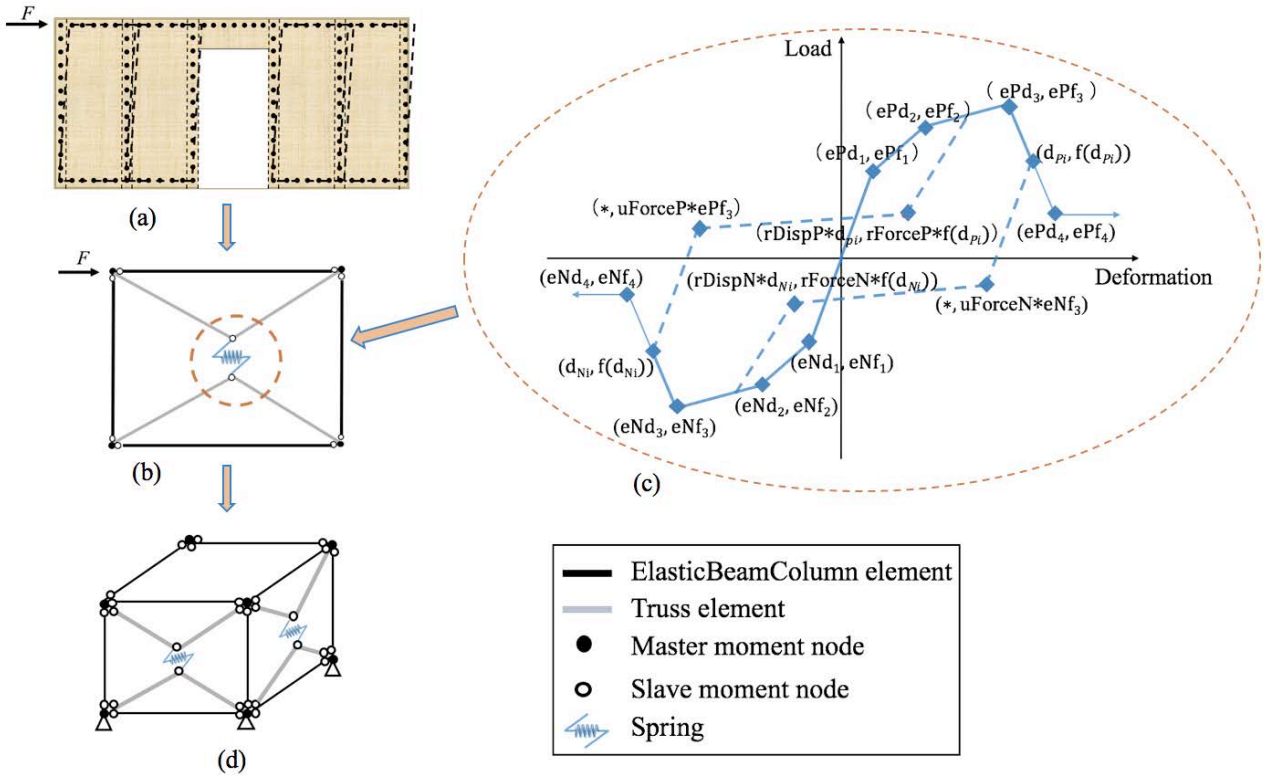

Fig. 4 A simplified approach for LFWB, (a) sketch of a single shear wall, (b) the simplified model of a single shear wall, (c) Pinching4 model, (d) 3D sketch of the LFWB

The modeling concept for a single shear wall is then extrapolated to the 3D structure, as shown in Fig. 4(d), consisting of a slab system and four shear walls. The slab system is assumed sufficiently stiff, and a multipoint is adopted to keep the same horizontal displacement of a floor. Four spring elements are created to simulate the shear wall of each direction. In Fig. 4d, only two spring elements are presented while the other two springs that cannot be seen from the view of paper are not plotted for clear expression. However, the way to create the model of LFWB inevitably induces some model errors, resulting from neglecting the interaction between components and simplified modeling assumptions, which may affect the accuracy of response prediction.

4. Seismic performance evaluation for LFWB

4.1 Model updating for the FE model using CKF

During the estimation process, how to select the identified parameters is a crucial issue because too many parameters may bring about the computation burden, whereas a few parameters have little effect on the estimated result. Initially, all 39 parameters of "Pinching4" are changed to find the tendency of root mean square error (RMSE). The RMSE measures model error between test result and model prediction. The comparison results show that the pinching and unloading/reloading parameters have little influence on the value of RMSE for the reason that these parameters are independent of the model details. A similar trend is also found in [15][16]. As a consequence, constant values assigned to these parameters are summarized in Table 1, and the remaining 16 parameters are chosen to be identified, as presented in Table 2. The procedure of model updating using CKF is introduced to update the FE model of LFWB. Fig. 5 compares the estimated time-history force with test response, in which the prediction response generating from all the cubature points covers the test result.

Table 1 Constant values of Pinching4 model

Parameter	Value	Parameter	Value	Parameter	Value	Parameter	Value
gK1	1	gD1	0.5	gF1	1	rForceP	0.28
gK2	0.5	gD2	0.5	gF2	0	rForceN	0.22
gK3	0.5	gD3	1	gF3	1	uForceP	0.05
gK4	0.5	gD4	1	gF4	1	uForceN	0.05
gKLim	0.25	gDLim	0.05	gFLim	0.001	dmgType	energy
gE	10	rDispP	0.8	rDispN	0.8		

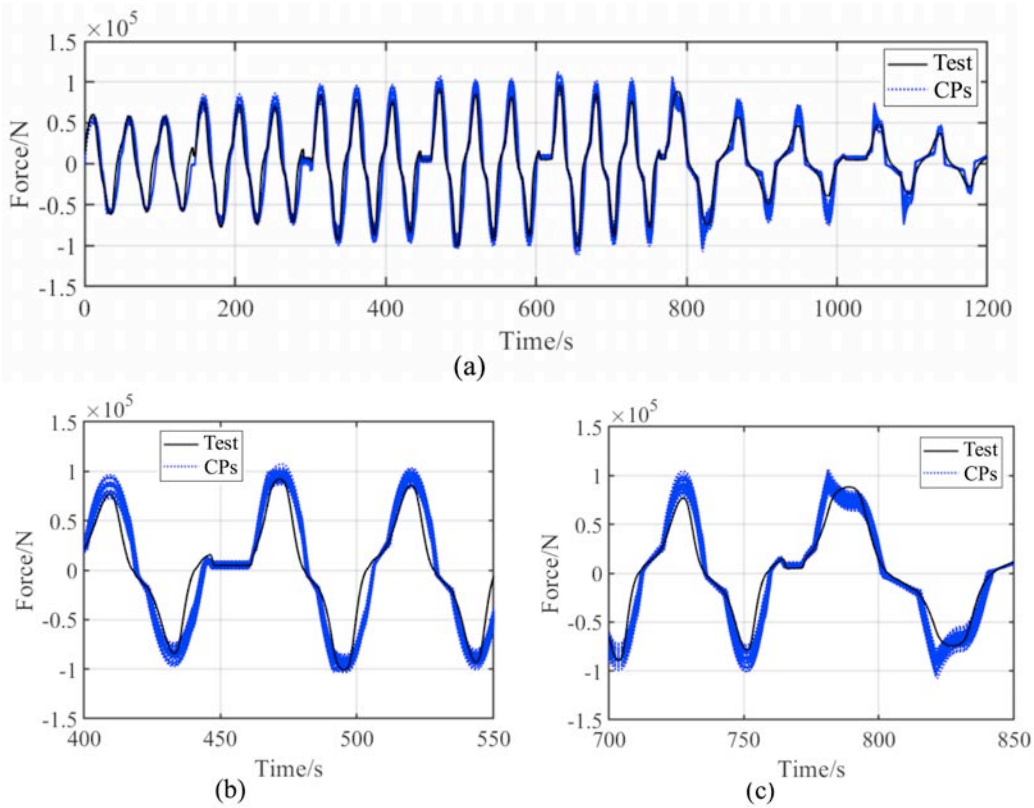

Fig. 5 Time-history of the estimated force: (a) the whole time history; (b) magnified view of time history 400s-550s; (c) magnified view of time history 700s-850s

Table 2 the identified model parameters

Parameter	Value	Parameter	Value	Parameter	Value	Parameter	Value
ePf1/N	18.65e3	eNf1/N	-25.57e3	ePd1/m	7.04e-3	eNd1/m	1.35e-2
ePf2/N	43.14e3	eNf2/N	-47.26e3	ePd2/m	2.91e-2	eNd2/m	4.48e-2
ePf3/N	47.68e3	eNf3/N	-50.72e3	ePd3/m	4.57e-2	eNd3/m	6.71e-2
ePf4/N	22.99e3	eNf4/N	-18.30e3	ePd4/m	9.31e-2	eNd4/m	1.2e-1

Table 2 summarizes the identified model parameters. When these parameters are regarded as input for the FE model, the hysteric curve, as well as the backbone curve, can be generated. Fig. 6 compares of the hysteretic curve and backbone curve between test and model. A good agreement can be seen before the maximum load, where the main feathers of the hysteretic curve, including pinching, stiffness, and strength

degradation, are well grasped. After reaching the maximum capacity, some obvious difference between test and model are exhibited. It is likely that the test curve shows random drops because of nails failure and wood degradation, while the FE model follows a linear degradation that is not capable of capturing the above test phenomenon.

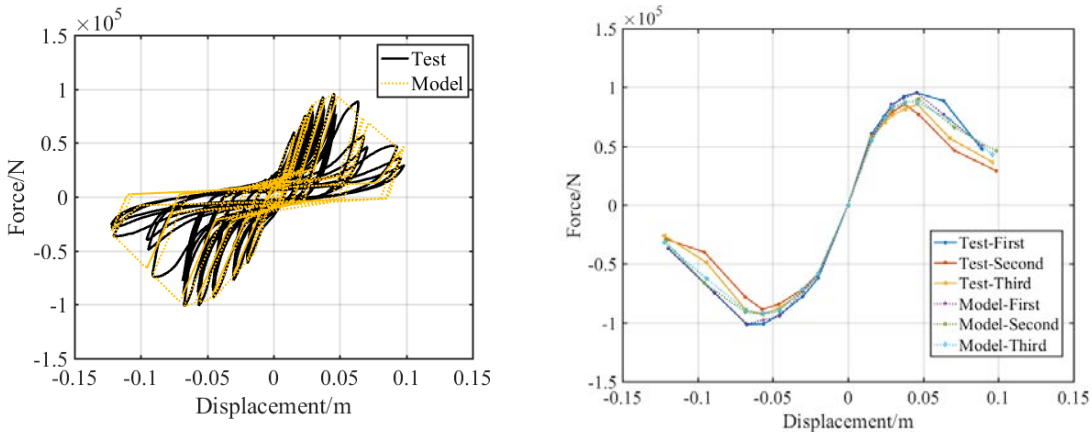

Fig. 6 Comparison of test and model, (a)hysteresis curve, (b)backbone curve

4.2 Seismic performance evaluation for LFWB

The updated FE model of LFWB is utilized to analysis hereafter. With the objective of assessing the seismic performance for different configurations of LFWB, six models ranging from one story to six-story are built by assembling different numbers of the calibrated model, as displayed in Fig. 7. These models are composed of slab systems and lateral resisting shear walls, whose slab system is assumed rigid diaphragm and the shear walls are modeled by the spring elements. A uniform distribution for the gravity loads with the value of 2kN/m^2 is assumed. The Rayleigh damping, including both tangent stiffness and mass proportional damping with a damping ratio of 5% is designated to the first and third modes.

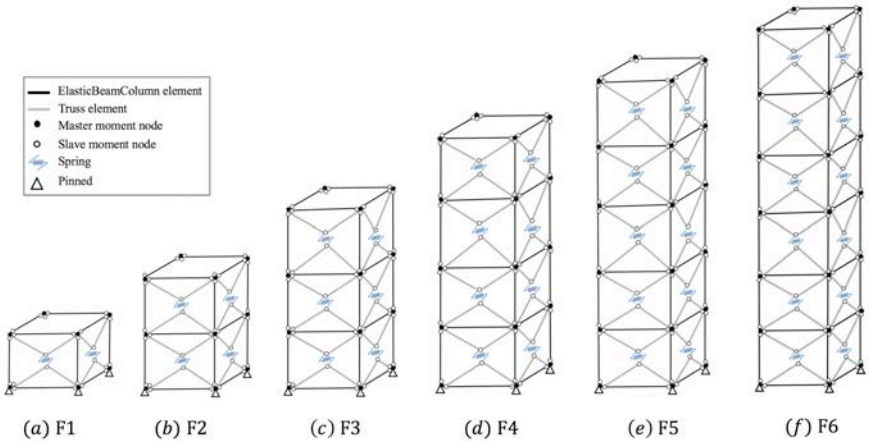

Fig. 7 Different configurations of LFWB

According to the FEMA 356 guideline [17], the maximum drift ratio is chosen to assess the structural performance levels, including immediate occupancy (IO), life safety (LS) and collapse prevention (CP). These three performance levels are corresponding to 1%, 2%, and 3% of the maximum drift ratio, respectively. The incremental dynamic analysis contains the necessary information to assess the above three performance levels, involving multiple nonlinear dynamic analyses of a structure subjected to a suite of earthquake records. Twenty-two pairs of far-field ground motion records recommend by FEMA 695 [18] are extracted from the PEER ground motion database [19]. To describe the scaling of earthquake records, the

spectral acceleration (S_a) at the fundamental period of structure is considered as the earthquake intensity measure (IM), where the spectra acceleration of the selected earthquake records is presented in Fig. 8.

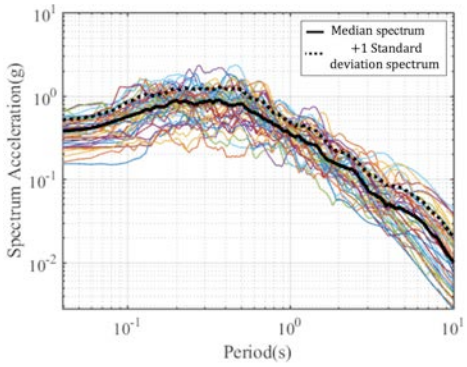

Fig. 8 Earthquake spectra of forty-four far-field record sets

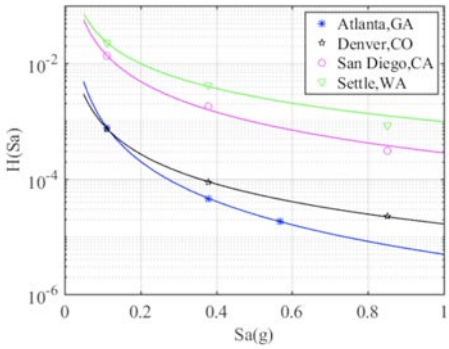

Fig. 9 Comparison of the seismic hazard of four cities in the US

When the above-described 44 earthquake records are applied to the six models, linearly scaled with a factor varying from 0.1 to 4 with a constant increment step of 0.1. The fragility function for different damage state levels is calculated by fitting a lognormal distribution to the spectral accelerations extracted from the IDA curves. The uncertainties in seismic demand σ_θ is calculated as the dispersion in θ, whereas the uncertainties in structural capacity β_{SC} is set equal to 0.25, 0.25 and 0.15 for IO, LS and CP limit states, respectively [20]. The fragility curves of each performance level are presented in Fig. 10, verifying that the median fragility reduces with the increase of height.

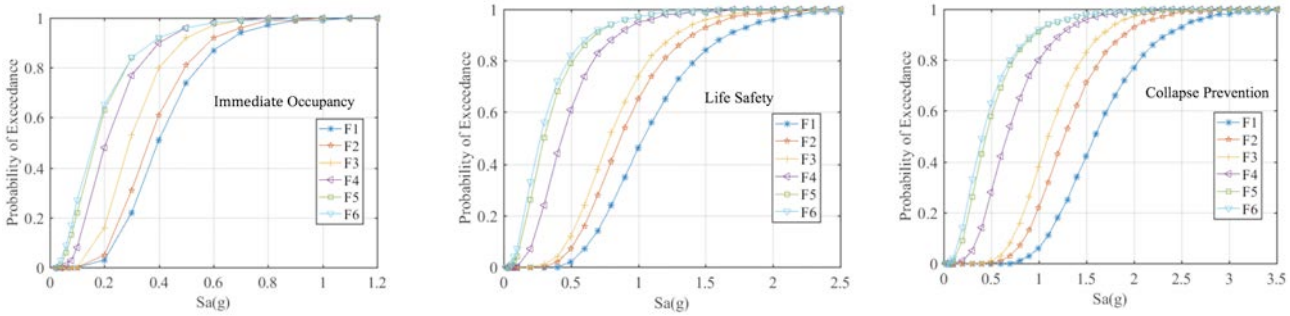

Fig. 10 Fragility curve for different configurations of LFWB

To consider the effect of seismic hazard region on the seismic risk assessment, four sites are selected, including Atlanta, GA; Denver, CO; San Diego, CA and Settle, WA. Fig. 9 compares the mean seismic hazard curves for a structure on the rock with a fundamental period of 0.4 seconds, in which k_0 and k are determined by least-squares analysis of the tabulated data from the US Geological Survey[21]. It can be seen that the annual probability of exceedance in the regions of San Diego and Settle are much larger than those in the Atlanta and Denver zones.

The seismic hazard curves represent the basis of mean earthquake occurrence rates for four typical sites. When they are incorporated with the fragility curves, the calculated annual probability of exceedance of different performance limit states for the LFWB is shown in Fig. 11. The limit state probability is obviously higher in the San Diego and Seattle regions than those in the zones of Atlanta and Denver. Because the two areas of San Diego and Seattle are in the high-seismic regions while the other two areas are moderate-seismic zones. The limit state probability raises with the building height increasing, especially when the story

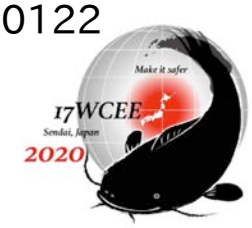

of LFWB is over than three, the annual exceeding probability for all three damage levels show noticeable increasing.

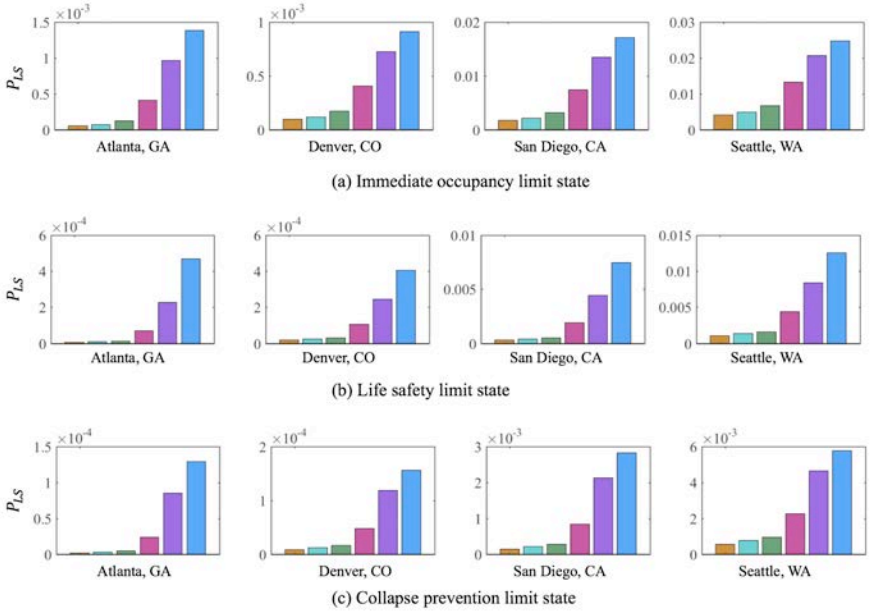

Fig. 11 Annual exceeding probability (P_{LS}) of different limit states at four cities in the US

5. Conclusions

Seismic risk assessment is essential for loss expectation and public decision-making. This paper puts forward the framework of probability seismic assessment conjoined with model updating technique. The model updating technique employing the CKF method performs a rigorous probability manner to identify the model parameters. The CKF method based on fifth-degree spherical-radial cubature rule is to estimate the mean and covariance of model parameters within the Gaussian filtering framework using available experimental data. When implementing the model updating for an FE model, the calibrated FE model is obtained, which is then utilized to evaluate the seismic performance. The performance is assessed based on the probabilistic seismic evaluation, including the fragility analysis and the limited state analysis. The fragility analysis gives the probability of exceeding a structural damage level using multi-record incremental dynamic analyses, associated with the uncertainties in seismic demands and the nonlinear characteristic of structures whereas the limit state probability analysis incorporated with the influence of seismic hazard region is to quantify the annual exceedance probability of a specified damage level.

The proposed framework is then applied to the case study of LFWB. A simplified FE model whose nonlinearity is governed by the spring element is modeled based on the test result. The CKF method that characterizes modeling uncertainties associated with the underlying structural system is employed to update the FE model. Compared to the hysteretic curve and backbone curve, there is a good agreement between the model and test, showing the identified parameters having a reasonable accuracy. Based on the updated model, different configurations ranging from one story to six-story are built. Then the fragility analysis and the limited state analysis serves an effective tool to evaluate the seismic performance. The analysis results show that the median fragility reduces with the height increases, and different seismic zones have a significant influence on the limit state probability analysis. The obtained information can be further utilized to loss estimation and expand the knowledge of engineering decision-making for seismic risk assessment.

6. References

[1] Kircher, C. A., Reitherman, R. K., Whitman, R. V., & Arnold, C. (1997). Estimation of earthquake losses to buildings. *Earthquake spectra*, **13**(4), 703-720.

[2] Ellingwood, Bruce R., David V. Rosowsky, and Weichiang Pang (2008): Performance of light-frame wood residential construction subjected to earthquakes in regions of moderate seismicity. *Journal of structural engineering*, **134.8**: 1353-1363.

[3] Berto, L., Saetta, A., & Simioni, P. (2012). Structural risk assessment of corroding RC structures under seismic excitation. *Construction and building materials*, **30**, 803-813.

[4] Cao, J., Xiong, H., & Chen, L. (2020). Procedure for parameter identification and mechanical properties assessment of CLT connections. *Engineering Structures*, **203**, 109867.

[5] Beck, J. L. (2010). Bayesian system identification based on probability logic. *Structural Control and Health Monitoring*, **17**(7), 825-847.

[6] Cheung, S. H., & Beck, J. L. (2009). Bayesian model updating using hybrid Monte Carlo simulation with application to structural dynamic models with many uncertain parameters. *Journal of engineering mechanics*, **135**(4), 243-255.

[7] Xu, B., Zhang, P., Wen, H., & Wu, X. (2016). Stochastic stability and performance analysis of cubature Kalman filter. *Neurocomputing*, **186**, 218-227.

[8] Cao, J., Xiong, H., Wang, Z., & Chen, J. (2020). Experimental investigation and numerical analysis for concrete-CLT connections. *Construction and Building Materials*, **236**, 117533.

[9] Campbell R, Hardy G, Merz K (2002). Seismic fragility application guide. Final report TR-1002988, EPRI, Palo Alto.

[10] Cornell, C. A., Jalayer, F., Hamburger, R. O., & Foutch, D. A. (2002). Probabilistic basis for 2000 SAC federal emergency management agency steel moment frame guidelines. *Journal of structural engineering*, **128**(4), 526-533.

[11] Jiahua, Kang (2012). Performance and Design Methodology Study on the Wood Framed Construction, PhD thesis 2012, Tongji University, China

[12] ASTM. (2012). Standard test methods for cyclic (reversed) load test for shear resistance of vertical elements of the lateral force resisting systems

[13] Mckenna F (2011). OpenSees: A Framework for Earthquake Engineering Simulation. *Computing in Science & Engineering*, **13**(4):58-66.

[14] Mitra N. (2012), Pinching4 model (OpenSees User Documetation) <http://opensees.berkeley.edu/wiki/index.php/Pinching4_Material>.

[15] Rahmanishamsi, E., Soroushian, S., & Maragakis, M. (2016). Cyclic shear behavior of gypsum board-to-steel stud screw connections in nonstructural walls. *Earthquake Spectra*, **32**(1), 415-439.

[16] Cao, J., Xiong, H., Chen, J., & Huynh, A. (2019). Bayesian parameter identification for empirical model of CLT connections. *Construction and Building Materials*, **218**, 254-269.

[17] FEMA, 356 (2000): Prestandard and commentary for the seismic rehabilitation of buildings. Federal Emergency Management Agency, Washington, DC.

[18] FEMA, 695 (2009): Quanti cation of Building Seismic Performance Factors. Federal Emergency Management Agency, Washington, DC.

[19] PGMD; 2011. <http://peer.berkeley.edu/peer_ground_motion_database/>.

[20] Ellingwood, B. R., & Kinali, K. (2009). Quantifying and communicating uncertainty in seismic risk assessment. Structural Safety, 31(2), 179-187.

[21] USGS. <http://earthquake.usgs.gov>.